HNUE JOURNAL OF SCIENCE DOI: 10.18173/2354-1059.2022-0040
Natural Sciences, 2022, Volume 67, Issue 3, pp. 52-59
This paper is available online at http://stdb.hnue.edu.vn

MOLECULAR DYNAMICS SIMULATION OF MICROSTRUCTURAL CHANGE OF $Cu_{0.6}Ni_{0.2}Fe_{0.2}$ ALLOY DURING THE COOLING PROCESS

Nguyen Thi Thao and Nguyen Thi Thanh Thanh
Faculty of Physics, Hanoi National University of Education

Abstract. Molecular dynamic simulation has been used to study the microstructural change of $Cu_{0.6}Ni_{0.2}Fe_{0.2}$ consisting of 8788 atoms (5272 Cu, 1758 Ni, and 1758 Fe atoms) during the cooling process. The influence of temperature on the microstructural properties is studied in detail through the atomic potential energy, the radial distribution function, the number of types of atoms present in the sample, the distribution of coordination number, and simplex distribution. Simulation results indicate that a crystalline phase transition occurs when the sample was cooled. The range of transition temperature is the range at which the atomic potential energy changes dramatically. This sample consists of face-centered cubic (fcc) and hexagonal closed packed crystals alternated with amorphous structures. The number of the simplex with radii larger than 1.9 Å decreased rapidly as the sample changed to a crystalline state.

Keywords: MD, CuNiFe alloys, crystals, simplexes.

1. Introduction

FeCuNi alloys with good magnetic properties are important systems in studies of materials and condensed system physics [1]. The microstructural and mechanical properties of Cu-rich clusters in FeCuNi alloys have been studied extensively [2-5]. The effect of Cu precipitation on the tensile properties of these alloys was studied experimentally and simulated [6-8]. The addition of Ni atoms to the Fe-Cu alloy can increase the rate of nucleation and the density of Cu atoms [9-10]. The effect of Cu precipitation on the mechanical properties of $Fe_{1.1}$-$Cu_{0.9}$-Ni trivalent alloy at different temperatures was investigated [11]. The influence of the concentration of Cu and Ni atoms on the microstructure and magnetic properties of FeCuNi alloys has been studied both theoretically and experimentally [12]. The results show that the temperature of glass transition increase with the increase of the concentration of Ni atoms. The crystal structure formed is the fcc structure. The rapid cooling process to obtain the amorphous or crystalline structure of $Fe_{70}Cu_{15}Ni_{15}$nanodroplets was investigated [13].

Received October 14, 2022. Revised October 24, 2022. Accepted October 31, 2022.
Contact Nguyen Thi Thao, e-mail address: ntthao.hnue@gmail.com

Interestingly, all the frozen nanoparticles formed had a core-shell structure with Cu atoms on the surface.

The temperature of the phase transition increase with the size of these nanoparticles. The phase transition in the cooling process of FeCuNi alloys with a large concentration of Cu atoms has not been studied. Therefore, this paper investigates the structural change in the cooling process ofFeCuNi alloys with a concentration of Cu atoms of 60% through specific analysis of the coordination number, and the voids of different types of atoms.

2. Content

2.1. Computational procedures

Molecular dynamics simulations have been used to study the microstructural transition of $Cu_{0.6}Ni_{0.2}Fe_{0.2}$ alloy consisting of 8788 atoms (5272 Cu, 1758 Ni, and 1758 Fe atoms) during the cooling process. We used the Sutton-Chen (SC) type potential to describe atomic interactions. The form of the total energy of atoms is given by,

$$U_{tot} = \sum_i U_i = \sum_i \left[\frac{1}{2} \sum_{j \neq i} \left(\varepsilon_i \varepsilon_j \right)^{1/2} \left(\frac{(\alpha_i + \alpha_j)}{2 r_{ij}} \right)^{\frac{(n_i + n_j)}{2}} - c_i \left(\varepsilon_i \varepsilon_i \right)^{1/2} \left(\sum_{i \neq j} \left(\frac{(\alpha_i + \alpha_j)}{2 r_{ij}} \right)^{\frac{(m_i + m_j)}{2}} \right)^{1/2} \right] \quad (1)$$

where r_{ij} is the distance between atoms i and j, α is a length parameter scaling to the lattice spacing of the crystal, c is a positive dimensionless parameter, ε is a parameter with the dimensions of energy, and n, m are positive integers. These potential parameters are given in Table 1 [14].

Table 1. Parameters for the SC potential [14]

	$\varepsilon(10^{-2}eV)$	α(Å)	C	M	N
Cu	1.2391	3.615	39.755	6	9
Ni	1.5707	3.515	39.432	6	9
Fe	2.2022	3.485	28.847	8.1447	8.7932

The sample was initially heated at a temperature of 2000 K and pressure of 0 GPa for 100 ps. This sample then underwent two cooling processes from 2000 K to 300 K. In the first process, it was cooled from 2000 K to 1200 K with a cooling rate of 10^{12} K/s, then the rest it was cooled down to 300 K with a cooling rate of 4 x 10^{11} K/s. The method of common neighbor analysis (CNA) was used to analyze the structure of the system during the cooling process [15]. Atoms are considered neighboring atoms when the distance between them is less than the cut-off radius defined as the first minimum after the peak of the pair RDF (Radial Distribution Function).

The simplex consists of 4 four neighboring atoms that form a tetrahedron. The circum-sphere (CS) of this tetrahedron does not contain the coordinate of any atoms inside it [16]. The radius of the simplex, R_S, is also the radius of CS. Four atoms of the simplex form a cage around a spherical void. So the porosity of the sample can be

evaluated through the size and the distribution of simplexes. There are seven types of simplex in the CuNiFe sample: Cu, Ni, Fe, Cu-Ni, Cu-Fe, Ni-Fe, and Cu-Ni-Fe simplexes.

2.2. Results and discussion

When the sample is cooled from 1400 K to 300 K with the cooling rate of 4 x 10^11K/s, there is a change in the potential energy as shown in Figure 1. The potential energy of this sample decreases suddenly in the range of temperature from 550 K to 400 K. This is the phase transition temperature range of the sample.

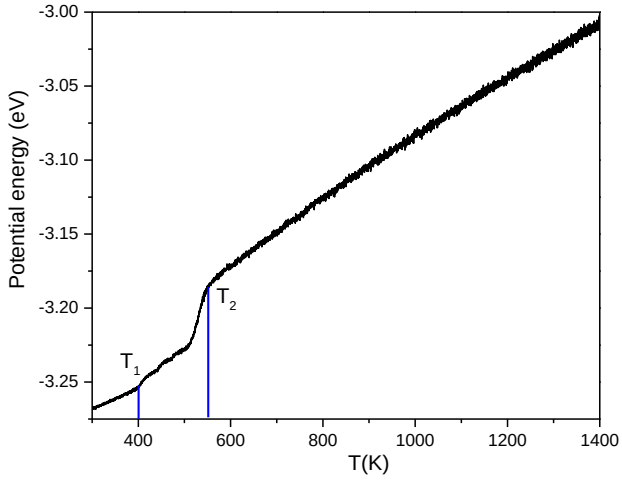

Figure 1. The variation of potential energy during the cooling process

The fraction of different types of atoms during the cooling process is pointed out in Figure 2.

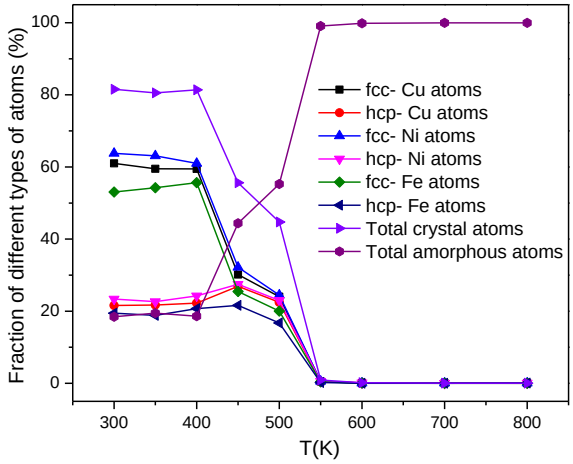

Figure 2. The fraction of different types of atoms as a function of the temperature

As the temperature decreases, the number of crystal atoms increases while one of the amorphous atoms decreases. The fraction of different types of atoms suddenly increases in the temperature range of 550 K - 400 K. In this temperature range, the structure of the sample changes from amophous state to a crystal state. At 300 K, the sample consists of 7165 crystal atoms (accounting for 81.53 %) with fcc and hcp structures. This structural change is also expressed through the transformation of the RDF of the sample as shown in Figure 3. At the temperature of less than 500 K, the sample has more ordered structures because there are more clear peaks at the large distance.

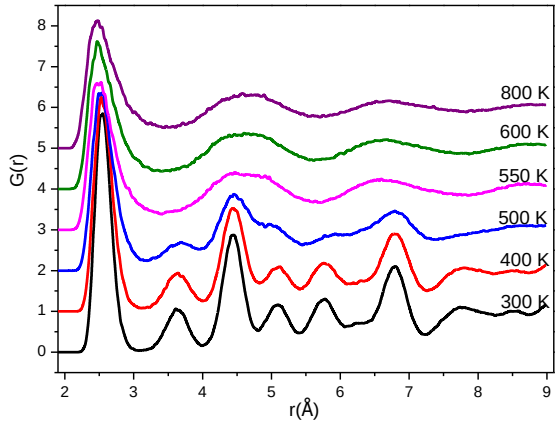

Figure 3. The partial RDF at different temperatures during the cooling process

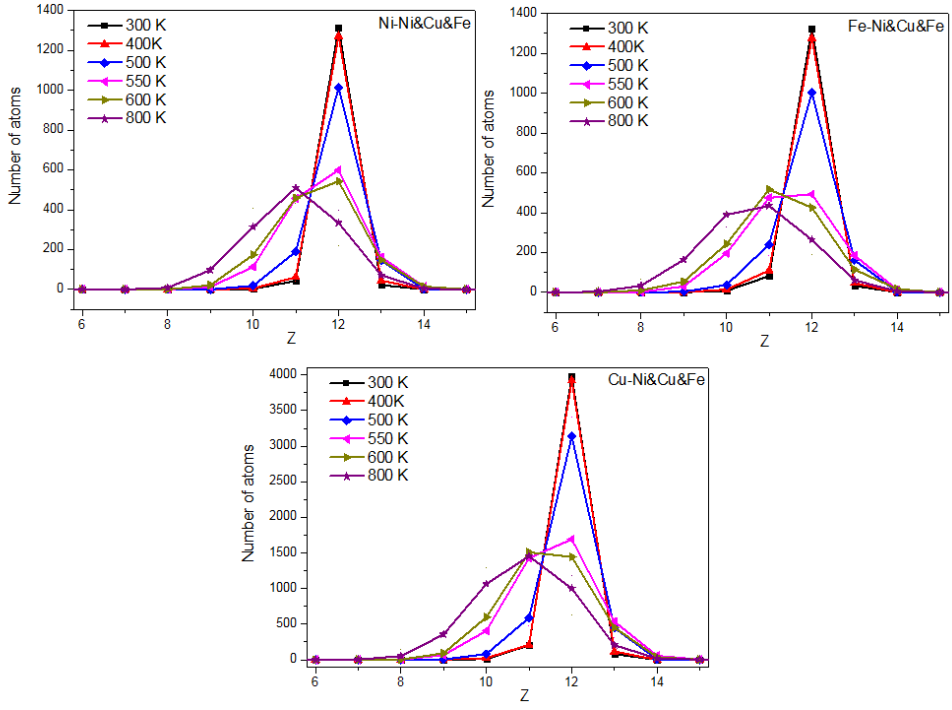

Figure 4. The coordination number (Z) distributions of Cu, Ni, and Fe atoms as a function of temperature

Figure 4 shows the distributions of the coordination number (Z) of Cu, Ni, and Fe atoms at different temperatures. At the temperature of 800 K, the peak of the coordination number locates at Z=9. In the range of temperature from 500 K to 300 K, the peak of the coordination number distribution locates at Z=12. When temperature decreases, the peak of this distribution narrows to the higher coordination number, indicating that neighbouring atoms are closer.

The structural change of the sample during the cooling process is visually observed in Figure 5. At 800 K, the amorphous structure spreads out the sample. As the temperature decreases, fcc and hcp phases dominate in the sample. We can observe the lattice arrangement of atoms in the sample at a temperature of 300 K. Fraction of the radii distributions of simplexes at different temperatures is shown in Figure 6. These distributions of the simplexes at 300 K have two peaks which locate at 1.575 and 1.775 Å. These peaks show that the atoms of the sample are only the fcc and hcp atoms. At higher temperatures, these peaks shift to the right and decrease the high. At a temperature of 800 K, the radii distribution has one peak at 1725 Å. Therefore, at high temperature, the number of these simplexes decreases and they become bigger. The radii of the simplexes in the crystalline structure (the range of temperature less than 550 K) are less than 1.9 Å whereas the number of the simplexes with $R_S \geq 1.9$ Å is significant at the temperature range of 550 - 800 K. We considered the big simplexes with $R_S \geq 1.9$ Å during the cooling process. The number of these big simplexes decreases with decreased temperature as presented in Figure 7. The number of big Cu-Fe simplexes decreases quickly with decreasing temperature. The big simplexes with $R_S \geq 1.9$ Å are visualized in Figure 8. At a temperature of 800 K, there are lots of big simplexes that form big clusters. As the temperature decreases, the number of big simplexes decreases.

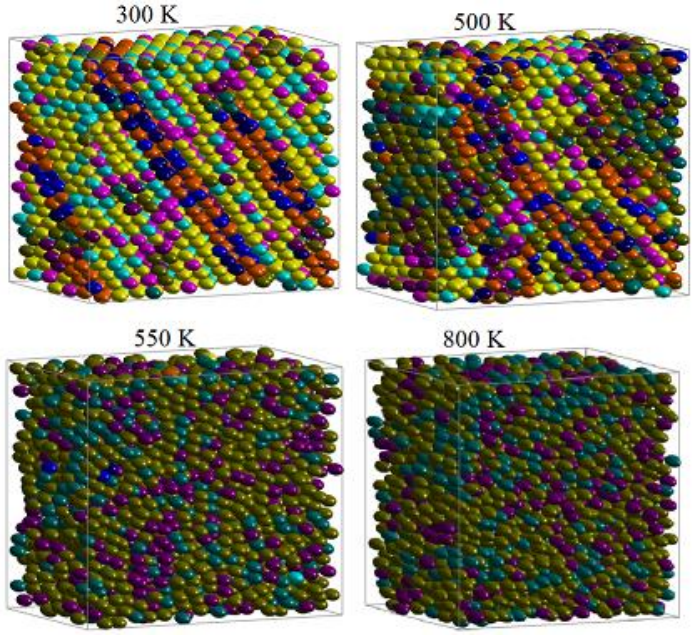

Figure 5. Cross-sectional $Cu_{60}Ni_{20}Fe_{20}$ sample under the cooling process

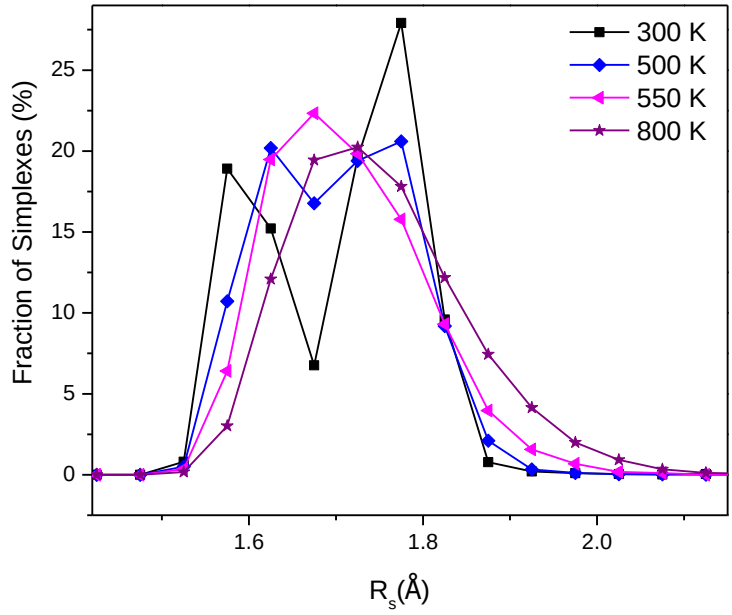

Figure 6. Fraction of radii distributions of the simplexes at different temperatures

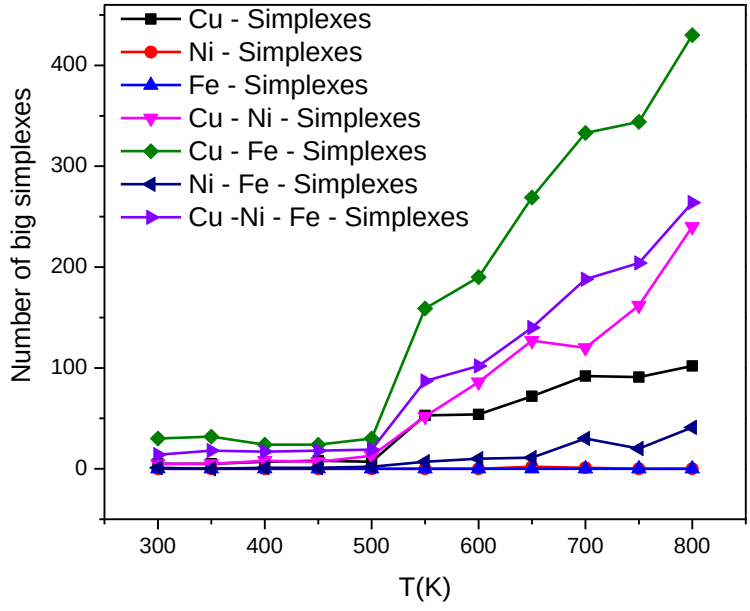

Figure 7. The number of big simplexes with Rs ≥1.9 Å as a function of the temperature

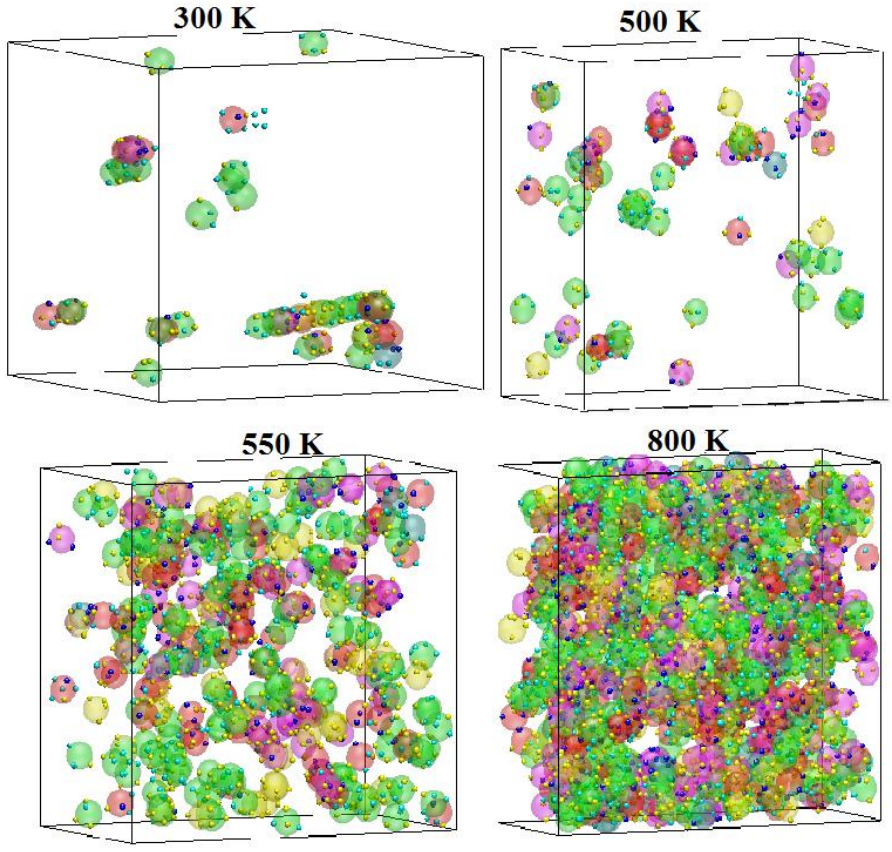

Figure 8. Visualization of big simplexes with $R_S \geq 1.9$ Å at different temperature

3. Conclusions

The $Cu_{0.6}Fe_{0.2}Ni_{0.2}$ alloy sample during the cooling process was studied by the Molecular dynamics simulation. At a temperature of 300 K, this sample contains 81.5% of fcc and hcp crystals. The temperature range of phase transition is from 550 K to 400 K. The number of big simplexes with $R_S \geq 1.9$ Å decreases rapidly in the region of the crystal structure. The number of Cu-Fe big simplexes is the largest and fastest decrease during the cooling process.

Acknowledgment. This research is funded by the Vietnamese Ministry of Education and Training project (B2020-SPH-01).

REFERENCES

[1] K. Suzuki, 1995. The role of non-crystalline structure in materials science. *J. Non-Cryst. Solid*, 193, 1-8.

[2] N. Castin, L. Malerba, G. Bonny, et al., 2009. Modeling radiation-induced phase changes in binary FeCu and ternary FeCuNi alloys using an artificial intelligence-based atomistic kinetic Monte Carlo approach. *Nucl. Instrum. Methods Phys. Res., B*, 267, 3002-3008.

[3] Y. Wang, J. Yin, X.B. Liu, 2017. Precipitation kinetics in binary Fe-Cu and ternary Fe-Cu-Ni alloys via KMC method. *Prog. Nat. Sci. Mater. Inter.*, 27, pp. 460-466.

[4] J. Li, Q.H. Fang, B. Lin, 2017. Twinning-governed plastic deformation in a thin film of body-centred cubic nanocrystalline ternary alloys at low temperature. *J. Alloys Compd*., 727, pp. 69-79.

[5] K. Liu, L.J. Hu, Q.F. Zhang, 2017. Effect of Ni and vacancy concentration on the initial formation of Cu precipitate in Fe-Cu-Ni ternary alloys by molecular dynamics simulation. *Chin. Phys. B*, 26, pp. 1-7.

[6] W.H. Zhou, H. Guo, Z.J. Xie, C.J. Shang, R.D.K. Misra, 2014. Cooper precipitation and its impact on mechanical properties in a low carbon micro alloyed steel processed by three-step heat treatment. *Mater. Des.*, 63, pp. 42- 49.

[7] I. Holzer, E. Kozeschnik, 2010. Computer simulation of the yield strength evolution in Cu-precipitation strengthened ferritic steel. *Mater. Sci. Eng., A*, 527, 3546-3551.

[8] L.J. Peng, B.Q. Xiong, G.L. Xie, Q.S. Wang, S.B. Hong, 2013. Precipitation process and its effects on properties of aging Cu–Ni–Be alloy. *Rare Met.*, 32, pp. 332- 337.

[9] A.T. Al-Motasem, M. Posselt, F. Bergner, U. Birkenheuer, 2011. Structure, energetics, and thermodynamics of copper-vacancy clusters in bcc-Fe: An atomistic study. *J. Nucl. Mater.*, 414, pp. 161-168.

[10] Y.P. Xie, S.J. Zhao, 2011. The energetic and structural properties of bcc NiCu, FeCu alloys: A first-principles study. *Comput. Mater. Sci*., 50, pp. 2586-2591.

[11] Li-Juan You, Li- Juan Hu, Yao-Ping Xie, Shi-Jin Zhao, 2016. *Comput. Mater. Sci.*, 118, pp. 236-244.

[12] A. Younes, N. Dilmi, M. Khorchef, et al., 2018. Structural and magnetic properties of FeCuNi nanostructured produced by mechanical alloying. *Appl. Surf. Sci.*, 446, pp. 258-265.

[13] Xuan Li, Zean Tian, Quan Xie, Kejun Dong, 2021. The topologically close-packed $Fe_{70}Cu_{15}Ni_{15}$ nanoparticles - A simulation study. *Vacuum* Volume 193, November, 110523.

[14] A. P. Sutton and J. Chen, 1990. Long-range Finnis–Sinclair potentials. *Philosophical Magazine Letters*, 61(3):139-146.

[15] FakenD, JonssonH, 1994. Systematic analysis of local atomic structure combined with 3D computergraphics. *Comput. Mater. Sci.*, 2: 279.

[16] Le VV, Lien L T H, 2021. Structural and mechanical properties of densified $(Li_2O)_{0.2}(SiO_2)_{0.8}$ glasses: A molecular dynamics simulations study. *J. Non-Cryst. Solids*; 564: 120840.